Distributed Control of Active Distribution Networks to Support Voltage Control in Subtransmission Networks*

Zhiyuan Tang[a,*], David J. Hill[b,c], Tao Liu[b]

[a]Department of Electrical and Computer Engineering, University of Waterloo, Canada
[b]Department of Electrical and Electronic Engineering, The University of Hong Kong, Hong Kong
[c]School of Electrical and Information Engineering, The University of Sydney, NSW 2006, Australia

Abstract

Utilizing highly distributed energy resources (DERs) dispersed in distribution networks is attracting recent attention as an effective solution to support voltage control in subtransmission networks. However, a subtransmission network usually has a large number of DERs within a small number of distribution networks. It is impractical to control these DERs directly by the subtransmission voltage controller (STVC). To solve this challenge, each distribution network with DERs is treated as a distributed energy resource cluster (DERC) and serves as the intermediary between DERs and the STVC. The primary objective of each DERC is to rapidly follow the active power change command given by the STVC. However, due to the high R/X ratio of lines in distribution networks, the active power changes of DERs can also lead to serious power quality issues. To overcome these issues, this paper develops a novel distributed control framework for DERCs. The proposed control framework consists of two modules: a command following module and a power quality management module. The former one aims to rapidly track the active power change command from the STVC by coordinating the active power of DERs in an optimal distributed manner. The latter one aims to improve the power quality by coordinating both the active and reactive power of DERs also in an optimal distributed manner. The effectiveness of the proposed control framework is tested through a modified IEEE 30-bus test system.

Keywords: Distributed control, active distribution network, distributed energy resources, voltage support, subtransmission network

1. Introduction

Traditionally, voltage variations in a subtransmission network are caused by slow load changes, which are handled by controlling on-load tap changers (OLTCs) and capacitors. However, with the integration of distributed wind farms at subtransmission levels, the voltage variations become fast and significant due to the inherent variability and intermittence of wind power. As a consequence, OLTCs and capacitors may undergo an excessive number of operations [1]. Moreover, in some cases, OLTCs and capacitors may be not fast enough to achieve certain control objectives due to their discrete control nature [1]. To solve these challenges, some flexible controllers with fast responses are required [2].

Due to the spatial distribution and fast responses, the option of using highly distributed energy resources (DERs) scattered in distribution networks has gained a lot of attention [3, 4, 5]. However, in a subtransmission network, there usually are huge numbers of DERs within a small number of distribution networks. It is impractical and even impossible to control them directly by the subtransmission voltage controller (STVC). To solve this challenge, we regard each distribution network with DERs as a distributed energy resource cluster (DERC) which serves as an intermediary between DERs and the STVC. The function of DERC is to aggregate a cluster of DERs in the corresponding distribution network and create a single entity to the STVC. It is similar to the function of load aggregators proposed in [3] and the virtual power plants used in [4, 5].

In our previous work [3, 4, 5], we focused on the coordination of DERCs from a subtransmission operator's view and the design of coordinated control schemes for DERCs to provide flexible voltage support for subtransmisson networks. Particularly, in [3], the coordination of DERCs with conventional regulation devices such as OLTCs and capacitors was considered. In this paper, we focus on the detailed management scheme for each DERC and aim to develop a general coordinated control framework for all DERs to support the voltages via the DERC.

For each DERC, the primary objective is to rapidly follow the active power change command given by the STVC. However, due to the high R/X ratio of lines in distribution networks, active power changes of DERs may cause serious

*This work was fully supported by the Research Grants Council of the Hong Kong Special Administrative Region under the Theme-based Research Scheme through Project No. T23-701/14-N.

*Corresponding author
Email address: zhiyuan.tang@uwaterloo.ca (Zhiyuan Tang)

power quality issues such as significant voltage variation, serious voltage violation, and increased network losses in the distribution network. To solve these issues, we propose a novel control framework for each DERC. The control framework consists of two modules: a command following module and a power quality management module. The former one aims to rapidly track the active power change command from the STVC by coordinating the active power of DERs, and the latter one aims to guarantee the power quality by coordinating both the active and reactive power of DERs.

Usually, the coordination of DERs at distribution levels is realized in a centralized manner by solving a network-wide optimal power flow problem (e.g. [6, 7, 8]). However, such a centralized method lacks scalability to incorporate the increasing number of DERs in distribution networks [9]. Another approach for controlling DERs is the local-policy based method that requires no communication at all (e.g. [10, 11, 12]). However, such a local-policy based framework lacks coordination and usually achieves a suboptimal solution, i.e., the full potential of DERs is not exploited in these local-policy based strategies [9, 10]. There also exist distributed control strategies that coordinate DERs in the network via information exchange among neighboring buses (e.g. [9, 13, 14, 15, 16]). In [13], based on dual ascent method, a distributed feedback control algorithm is proposed to regulate voltages in the network. In [14], based on accelerated gradient method, a fast distributed control scheme is developed to coordinate DERs in distribution networks for voltage regulation. In [16], based on alternating direction method of multiplier (ADMM), DERs in the network are coordinated to minimize the total power losses. However, all of these works did not consider the problem of how to coordinate DERs in distribution networks to provide ancillary services for networks with higher voltage level. To overcome these issues, in this paper, we develop a distributed control framework for each DERC, i.e., both the command following and power quality management modules are realized in an optimal distributed manner, which can achieve optimal solutions only by requiring local communication between neighboring DERs. This framework can facilitate plug-and-play operations for the increased number of DERs and simplify their integrations into the DERC. The contributions of this paper are listed below:

- A general distributed control framework is proposed for DERCs to support voltage control in subtransmission networks. It is suitable in practice for its autonomy, flexibility, and scalability.
- The control problem of the command following module is converted into an equivalent restricted agreement problem, and is solved by a novel consensus-based algorithm in a distributed manner that has a fast convergence speed.
- The multi-objective control problem of the power quality management module is solved in a distributed manner based on a consensus version of ADMM.
- Through coordination of these two modules, each DERC can rapidly respond to the active power change command given by the STVC and guarantee the power quality within the DERC at the same time.

The rest of the paper is organized as follows. Section II introduces the distribution network model to be studied and the communication network used for information exchange between neighboring buses. The proposed distributed control framework is explicitly presented in Section III. A case study through a modified IEEE 30-bus system is given in Section IV. Conclusions are presented in Section V.

2. Network Description

2.1. Radial Distribution Network

Consider a single-phase connected radial distribution network with $N+1$ buses. Denote the bus set as $\mathcal{N} := \{0, 1, \ldots, N\}$ and the line set as $\mathcal{E} := \{(i,j)\} \subseteq \mathcal{N} \times \mathcal{N}$ that has N links representing the N line segments. Bus 0 denotes the point of common coupling (PCC), usually at the distribution substation. A radial distribution network illustration is given in Fig. 1. We assume that the active power change command from the STVC is sent to the PCC, i.e., bus 0. We also assume that each bus i, $i = 1, \ldots, N$ has one DER (e.g., distributed generator, storage device, or dispatchable load) with electronic interface that can change its active or reactive power output quickly [17, 18].

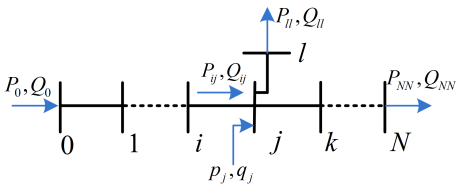

Figure 1: Schematic diagram of a radial distribution network

The DistFlow equations proposed in [19, 20] are employed to model the distribution network flow for each line $(i,j) \in \mathcal{E}$ as follows

$$P_{ij} - \sum_{k \in \mathcal{N}_j^d} P_{jk} = -p_j + r_{ij} \frac{P_{ij}^2 + Q_{ij}^2}{v_i^2} \tag{1a}$$

$$Q_{ij} - \sum_{k \in \mathcal{N}_j^d} Q_{jk} = -q_j + x_{ij} \frac{P_{ij}^2 + Q_{ij}^2}{v_i^2} \tag{1b}$$

$$v_i^2 - v_j^2 = 2(r_{ij} P_{ij} + x_{ij} Q_{ij}) - (r_{ij}^2 + x_{ij}^2) \frac{P_{ij}^2 + Q_{ij}^2}{v_i^2} \tag{1c}$$

where v_j, p_j, and q_j denote the voltage magnitude, active and reactive power injection of bus j, respectively; P_{ij}, Q_{ij} are the active and reactive power from bus i to bus j, respectively; r_{ij} and x_{ij} are the resistance and reactance of line segment (i, j), respectively; and the nonlinear term $(P_{ij}^2 + Q_{ij}^2)/v_i^2$ represents the squared line current magnitude that is associated with the loss term in (1a)-(1c). For convenience, we define $\mathcal{N}_j^a$ and $\mathcal{N}_j^d$ to denote bus j's one ancestral neighbor (e.g., $\mathcal{N}_j^a = \{i\}$ in Fig. 1) and all descendant neighbors (e.g., $\mathcal{N}_j^d = \{k, l\}$ in Fig. 1), respectively. In particular, for the bus l, $l \in \mathcal{T}$ where the set $\mathcal{T}$ consists of all the buses at the end of the branch in the network (e.g. $\mathcal{T} = \{l, N\}$ in Fig. 1), we define $\mathcal{N}_l^d = \{l\}$ and $P_{ll} = Q_{ll} = 0$, which is known as the terminal condition [19].

The LinDistFlow model proposed in [11] is adopted to linearize the DistFlow equations (1a)-(1c) by assuming the negligible line losses and almost flat voltage profile:

$$P_{ij} - \sum_{k \in \mathcal{N}_j^d} P_{jk} = -p_j \tag{2a}$$

$$Q_{ij} - \sum_{k \in \mathcal{N}_j^d} Q_{jk} = -q_j \tag{2b}$$

$$v_i - v_j = r_{ij} P_{ij} + x_{ij} Q_{ij}. \tag{2c}$$

The accuracy of the LinDistFlow model (2) has been verified by several recent works, see [9, 10] for examples. Although the LinDistFlow model (2) is adopted to design the distributed algorithms in this paper, the performance of the proposed distributed control framework for DERC has been verified by the case study where the full ac power flow model is adopted for lossy distribution networks.

2.2. Communication Network

As already mentioned, the whole control framework will be implemented in a distributed manner. For the required communication network, we assume that

1. The communication network has the same topology as the physical network.
2. There are undirected communication links between neighboring buses.

The above two assumptions are not conservative in practice and have been widely used in the literature (e.g. [9, 16]). Note that, in the proposed control framework, the command following and power quality management modules share the same communication network but with different information update algorithms.

3. Distributed control framework

3.1. Overview

In this paper, based on the LinDistFlow equations (2a)-(2c), a general distributed coordinated control framework is proposed for DERCs to support voltage control in sub-transmission networks. The proposed control scheme consists of two modules: a command following module and a power quality management module. These two modules are designed in a complementary way such that each DERC can rapidly respond to the active power change command given by the STVC without jeopardizing the power qualities within the DERC. The details of these two modules will be presented in Sections III-B and III-C, respectively. The extension to the three-phase unbalanced systems will be discussed at the end.

3.2. Command Following Module

This module aims to rapidly follow the active power change command given by the STVC by coordinating the active power of DERs in an optimal distributed manner. When DERs provide ancillary services to the grid, they should be paid compensation fees. Here, we assign a simple quadratic cost function $f_i(\Delta p_i)$ for the i^{th} DER, which is widely used in the literature (e.g. [21]):

$$f_i(\Delta p_i) = \frac{1}{2} a_i \Delta p_i^2 + b_i \Delta p_i \tag{3}$$

where $a_i > 0$ and $b_i \geq 0$ are the price coefficients which can be determined by bargaining between the STVC and DER owners through the electricity market.

Based on the cost function (3) and linearized active power flow equation (2a), we consider an optimal dispatch scheme for DERs. The objective is to minimize the total compensation fees paid by the STVC while satisfying the active power change command and local control limits. The optimization problem is given as follows:

$$\min \sum_{i=1}^{N} f_i(\Delta p_i),\ s.t.\ \sum_{i=1}^{N} \Delta p_i = \Delta p_{ref},\ \Delta \underline{p}_i \leq \Delta p_i \leq \Delta \overline{p}_i \tag{4}$$

for all $i = 1, \ldots, N$ where Δp_{ref} is the active power change command given by the STVC; Δp_i denotes the active power change needed at bus i; $\Delta \underline{p}_i$ and $\Delta \overline{p}_i$ are the lower and upper bounds for Δp_i, respectively.

To solve (4) in a distributed way, we first convert it to the following equivalent optimization problem by adding the active power change command Δp_{ref} received by the PCC into (4) as a new decision variable Δp_0 with a local constraint $-\Delta p_{ref} \leq \Delta p_0 \leq -\Delta p_{ref}$ (i.e., $\Delta \underline{p}_0 = \Delta \overline{p}_0 = -\Delta p_{ref}$):

$$\min \sum_{i=0}^{N} f_i(\Delta p_i) \tag{5a}$$

$$s.t.\ \sum_{i=0}^{N} \Delta p_i = 0 \tag{5b}$$

$$\Delta \underline{p}_i \leq \Delta p_i \leq \Delta \overline{p}_i,\ \forall i \in \mathcal{N} \tag{5c}$$

where $f_0(\Delta p_0) = \frac{1}{2} a_0 \Delta p_0^2 + b_0 \Delta p_0$ with $b_0 \geq 0$. The parameter a_0 will be selected later.

Based on the cost function in (5a), an incremental cost is introduced for each bus i:

$$\lambda_i = \frac{df_i}{d\Delta p_i} = a_i \Delta p_i + b_i, \ \forall i \in \mathcal{N}. \tag{6}$$

According to the first order optimality conditions of the optimization problem (5a)-(5c), the optimal solution $\Delta p_i^*, \ \forall i \in \mathcal{N}$ can be uniquely expressed with λ^*:

$$\Delta p_i^* = \mathcal{P}_i \left[\frac{\lambda^* - b_i}{a_i} \right] \tag{7}$$

where λ^* is the optimal incremental cost which is also the Lagrange multiplier associated with the active power balance equation in (5b), the notation $\mathcal{P}_i[\cdot]$ denotes the projection operator for bus i, i.e., it projects the argument into the local constraint $[\Delta \underline{p}_i, \Delta \overline{p}_i]$. Combining the active power balance constraint in (5b) and the optimal condition (7), the original optimization problem (5a)-(5c) (which is assumed to be solvable) is formed as the following restricted agreement problem:

$$\sum_{i=0}^{N} \Delta p_i^* = \sum_{i=0}^{N} \mathcal{P}_i \left[\frac{\lambda^* - b_i}{a_i} \right] = 0. \tag{8}$$

To solve (8) in a distributed manner as quickly as possible, we adopt the algorithm proposed in [21] which has a fast convergence speed. The communication network employed can be described as an undirected graph $\mathcal{G} = \{\mathcal{N}, \mathcal{E}, W\}$ where the communication weight matrix $W = (w_{ij}) \in R^{(N+1)\times(N+1)}$. If $(i,j) \in \mathcal{E}$, $i \neq j$, then $w_{ij} = w_{ji} > 0$ and $\sum_{j=1, i\neq j}^{N+1} w_{ij} < 1$; otherwise, $w_{ij} = w_{ji} = 0$. The diagonal entry w_{ii} of the matrix satisfies $w_{ii} = 1 - \sum_{j=1, i\neq j}^{N+1} w_{ij}$. Based on the communication network mentioned above, the update process for each bus i, $i \in \mathcal{N}$ is given as follows [21]:

$$\begin{aligned} \lambda_i(r+1) =& \lambda_i(r) + \sum_{j=0}^{N} w_{ij}\lambda_j(r) - \sum_{j=0}^{N} \tilde{w}_{ij}\lambda_j(r-1) \\ & - \alpha \left(\mathcal{P}_i \left[\frac{\lambda_i(r) - b_i}{a_i} \right] - \mathcal{P}_i \left[\frac{\lambda_i(r-1) - b_i}{a_i} \right] \right) \end{aligned} \tag{9}$$

whose first step performs the update $\lambda_i(1) = \sum_{j=0}^{N} w_{ij}\lambda_j(0) - \alpha \mathcal{P}_i \left[\frac{\lambda_i(0) - b_i}{a_i} \right]$. Here $\lambda_i(r)$ denotes the incremental cost of bus i at iteration r, $r = 0, 1, 2, \ldots$; $\tilde{w}_{ij}$ is the element of matrix $\tilde{W} = \frac{I+W}{2} \in R^{(N+1)\times(N+1)}$ (here, $I \in R^{(N+1)\times(N+1)}$ is the identity matrix). In order to guarantee the convergence of (9), the step size α should satisfy [21]:

$$0 < \alpha < 2\sigma_{min}(\tilde{W}) \min\{a_i\} \tag{10}$$

where $\sigma_{min}(\tilde{W})$ denotes the smallest eigenvalue of $\tilde{W}$ and $\min\{a_i\}$ denotes the smallest a_i, $i \in \mathcal{N}$. Once algorithm (9) converges, the optimal active power change for each bus i, $i = 1, \ldots, N$ can be calculated by (7).

In general, the larger α in algorithm (9) is, the faster the algorithm will converge. As mentioned earlier, to allow a distributed implementation, the active power change command Δp_{ref} received by bus 0 is added into the original optimization problem (4) as a new decision variable Δp_0 with associated cost function $f_0(\Delta p_0) = \frac{1}{2} a_0 \Delta p_0^2 + b_0 \Delta p_0$. In order to not decrease the value of α, based on (10), the cost coefficient a_0 should be selected such that $a_0 \geq \min\{a_i\}$, $i = 1, \ldots, N$.

3.3. Power Quality Management Module

Due to the high R/X ratio of lines in the distribution network, the active power changes of DERs caused by the command following module may cause serious voltage issues such as significant voltage variation, serious voltage violation, and increased network losses. To handle these issues, the power quality management module is proposed by coordinating both the active and reactive power of DERs.

In the proposed power quality management module, based on the linearized DistFlow equations (2a)-(2c), we consider the following optimization problem:

$$\min \sum_{(i,j)\in\mathcal{E}} r_{ij} \frac{P_{ij}^2 + Q_{ij}^2}{v_i^2} \tag{11a}$$

subject to equations (2a)-(2c) and the constraints:

$$\underline{v}_j \leq v_j \leq \overline{v}_j, \ j = 1, \ldots, N \tag{11b}$$

$$\underline{p}_j \leq p_j \leq \overline{p}_j, \ j = 1, \ldots, N \tag{11c}$$

$$\underline{q}_j \leq q_j \leq \overline{q}_j, \ j = 1, \ldots, N \tag{11d}$$

$$P_{01} = \bar{P}_0, Q_{01} = \bar{Q}_0, P_{ll} = 0, Q_{ll} = 0, \ l \in \mathcal{T} \tag{11e}$$

where the objective is to minimize the total power losses while guaranteeing that the voltage and power injections of DERs stay whithin the allowable ranges. The symbols $\underline{v}_j$ and $\overline{v}_j$ are the lower and upper voltage limits of bus j, respectively; $\underline{p}_j$ and $\overline{p}_j$ are the lower and upper limits of p_j, respectively; $\underline{q}_j$ and $\overline{q}_j$ are the lower and upper limits of q_j, respectively; $\bar{P}_0$ and $\bar{Q}_0$ are the original active and reactive power transmitted from the subtransmission network to the distribution network via PCC (bus 0) before activating the power quality management process, respectively. The conditions $P_{01} = \bar{P}_0$ and $Q_{01} = \bar{Q}_0$ in (11e) indicate that both the active and reactive power transmitted to the PCC from the subtransmission network should remain the same during the power quality management process, i.e. $\Delta P_0 = \Delta Q_0 = 0$ (refer to Fig. 1 for illustration). This is due to the fact that both the active and reactive power change of DERC (i.e., ΔP_0 and ΔQ_0) has an influence on the voltage regulation performance in the subtransmisson network due to the nonzero P/Q and V/Q sensitivity values [3, 5].

It is worth mentioning that minimizing the network losses can improve the control performance of the command following module. Since in the command following

module the linearized active power flow equation (2a) is adopted to design the dispatch problem (4) where the line loss is neglected, there will be a difference between the actual achieved active power change command and the expected one. So the smaller the network loss is, the more accurate the active power change command will be achieved.

In order to reformulate the above optimization problem as a convex quadratic program with linear constraints, we assume that the objective in (11a) can be approximated by $\sum_{(i,j)\in\mathcal{E}} r_{ij}\frac{P_{ij}^2+Q_{ij}^2}{v_0^2}$ under a relatively flat voltage profile [16]. Further, we observe that p_j can be uniquely determined by the active power flow through bus j, i.e., $P_{ij},\ i\in\mathcal{N}^a$ and $P_{jk},\ k\in\mathcal{N}^d$ (refer to (2a) and Fig. 1 for illustration), and q_j can be uniquely determined by the reactive power flow through bus j, i.e., $Q_{ij},\ i\in\mathcal{N}^a$ and $Q_{jk},\ k\in\mathcal{N}^d$ (refer to (2b) and Fig. 1 for illustration). Thus, the optimization problem (11a)-(11e) can be reformulated as an optimization problem where $\boldsymbol{P}=\{P_{ij}\},\ (i,j)\in\mathcal{E}$, $\boldsymbol{Q}=\{Q_{ij}\},\ (i,j)\in\mathcal{E}$ and $\boldsymbol{v}=\{v_j\},\ j=1,\ldots,N$ are the decision variables:

$$\min_{\boldsymbol{P},\boldsymbol{Q},\boldsymbol{v}} \sum_{(i,j)\in\mathcal{E}} r_{ij}\frac{P_{ij}^2+Q_{ij}^2}{v_0^2} \tag{12a}$$

subject to $\forall j=1,\ldots,N$:

$$v_j = v_i - \left(r_{ij}P_{ij}+x_{ij}Q_{ij}\right),\ i\in\mathcal{N}_j^a \tag{12b}$$

$$\underline{v}_j \le v_j \le \overline{v}_j \tag{12c}$$

$$\underline{p}_j \le \sum_{k\in\mathcal{N}_j^d} P_{jk} - \sum_{i\in\mathcal{N}_j^a} P_{ij} \le \overline{p}_j \tag{12d}$$

$$\underline{q}_j \le \sum_{k\in\mathcal{N}_j^d} Q_{jk} - \sum_{i\in\mathcal{N}_j^a} Q_{ij} \le \overline{q}_j \tag{12e}$$

$$P_{01}=\bar{P}_0, Q_{01}=\bar{Q}_0, P_{ll}=0, Q_{ll}=0,\ l\in\mathcal{T}. \tag{12f}$$

It can be seen from (12a)-(12f) that 1) the objective in (12a) can be separated into a sum of individual terms for each bus j and 2) the decision variables related to the constraints of bus j in (12b)-(12f) are only associated with its neighbors. Inspired by this particular structure, we adopt a consensus version of ADMM to solve the optimization problem (12a)-(12f) in a distributed manner. The ADMM has been widely used in the literature for its better convergence speed compared with other distributed solvers [16, 9]. The general discussion of ADMM can be found in [22].

To implement the ADMM update in a distributed manner for the optimization problem (12a)-(12f), we need to reformulate the optimization problem (12a)-(12f) as a consensus-based problem [9, 16]. To this end, we assign $2|\mathcal{N}_j^d|+4$ auxiliary variables (i.e., $\tilde{P}_{ji},\ i\in\mathcal{N}_j^a$, $\tilde{P}_{jk},\ k\in\mathcal{N}_j^d$, $\tilde{Q}_{ji},\ i\in\mathcal{N}_j^a$, $\tilde{Q}_{jk},\ k\in\mathcal{N}_j^d$, $\tilde{v}_{jj}$, and $\tilde{v}_{ji}, i\ \in\mathcal{N}_j^a$) to each bus j, which are used to locally estimate its own decision variables and the decision variables related to its neighbors. Then, the optimization problem (12a)-(12f) can be reformulated as follows:

$$\min_{\tilde{\boldsymbol{P}},\tilde{\boldsymbol{Q}},\tilde{\boldsymbol{v}}} \sum_{j=1}^{N} r_{ij}\frac{\tilde{P}_{ji}^2+\tilde{Q}_{ji}^2}{v_0^2} \tag{13a}$$

subject to $\forall j=1,\ldots,N$:

$$\tilde{v}_{jj} = \tilde{v}_{ji} - \left(r_{ij}\tilde{P}_{ij}+x_{ij}\tilde{Q}_{ji}\right),\ i\in\mathcal{N}_j^a \tag{13b}$$

$$\underline{v}_j \le \tilde{v}_{jj} \le \overline{v}_j \tag{13c}$$

$$\underline{p}_j \le \sum_{k\in\mathcal{N}_j^d} \tilde{P}_{jk} - \sum_{i\in\mathcal{N}_j^a} \tilde{P}_{ji} \le \overline{p}_j \tag{13d}$$

$$\underline{q}_j \le \sum_{k\in\mathcal{N}_j^d} \tilde{Q}_{jk} - \sum_{i\in\mathcal{N}_j^a} \tilde{Q}_{ji} \le \overline{q}_j \tag{13e}$$

$$\tilde{P}_{ji}=P_{ij},\ i\in\mathcal{N}_j^a, \text{ and } \tilde{P}_{jk}=P_{jk},\ k\in\mathcal{N}_j^d \tag{13f}$$

$$\tilde{Q}_{ji}=Q_{ij},\ i\in\mathcal{N}_j^a, \text{ and } \tilde{Q}_{jk}=Q_{jk},\ k\in\mathcal{N}_j^d \tag{13g}$$

$$\tilde{v}_{jj}=v_j, \text{ and } \tilde{v}_{ji}=v_i,\ i\in\mathcal{N}_j^a \tag{13h}$$

$$P_{01}=\bar{P}_0, Q_{01}=\bar{Q}_0, P_{ll}=0, Q_{ll}=0,\ l\in\mathcal{T} \tag{13i}$$

where $\tilde{\boldsymbol{P}}=\{\tilde{P}_{jk}\},\ k\in\mathcal{N}_j^a\cup\mathcal{N}_j^d$, $\tilde{\boldsymbol{Q}}=\{\tilde{Q}_{jk}\},\ k\in\mathcal{N}_j^a\cup\mathcal{N}_j^d$ and $\tilde{\boldsymbol{v}}=\{\tilde{v}_{jj},\tilde{v}_{ji}\},\ i\in\mathcal{N}_j^a,\ j=1,\ldots,N$. The conditions (13f)-(13h) enforce the agreement between each decision variable and its local auxiliary copy, which leads to the equivalence between optimization problem (12a)-(12f) and (13a)-(13i) [9, 16].

For the consensus-based optimization problem (13a)-(13i), its augmented Lagrangian function is formulated as $\mathcal{L}(\tilde{\boldsymbol{P}},\tilde{\boldsymbol{Q}},\tilde{\boldsymbol{v}})=\sum_{j=1}^{N}\mathcal{L}_j$ where

$$\mathcal{L}_j = r_{ij}\frac{\tilde{Q}_{ji}^2+\tilde{Q}_{ji}^2}{v_0^2} \tag{14a}$$

$$+\frac{\rho_P}{2}\left[\sum_{i\in\mathcal{N}_j^a}(\tilde{P}_{ji}-P_{ij})^2+\sum_{k\in\mathcal{N}_j^d}(\tilde{P}_{jk}-P_{jk})^2\right] \tag{14b}$$

$$+\frac{\rho_Q}{2}\left[\sum_{i\in\mathcal{N}_j^a}(\tilde{Q}_{ji}-Q_{ij})^2+\sum_{k\in\mathcal{N}_j^d}(\tilde{Q}_{jk}-Q_{jk})^2\right] \tag{14c}$$

$$+\frac{\rho_v}{2}\left[(\tilde{v}_{jj}-v_j)^2+\sum_{i\in\mathcal{N}_j^a}(\tilde{v}_{ji}-v_i)^2\right] \tag{14d}$$

$$
\begin{aligned}
&+\sum_{i\in\mathcal{N}_j^a}\lambda_{ji}^P(\tilde{P}_{ji}-P_{ij})+\sum_{k\in\mathcal{N}_j^d}\lambda_{jk}^P(\tilde{P}_{jk}-P_{jk})\\
&+\sum_{i\in\mathcal{N}_j^a}\lambda_{ji}^Q(\tilde{Q}_{ji}-Q_{ij})+\sum_{k\in\mathcal{N}_j^d}\lambda_{jk}^Q(\tilde{Q}_{jk}-Q_{jk})\\
&+\lambda_{jj}^v(\tilde{v}_{jj}-v_j)+\sum_{i\in\mathcal{N}_j^a}\lambda_{ji}^v(\tilde{v}_{ji}-v_i)
\end{aligned}
\tag{14e}
$$

where $\rho_P>0$, $\rho_Q>0$, and $\rho_v>0$ are the given penalty coefficients that are used to penalize the difference between the local estimates and the global variables; $\lambda_{ij}^P,\ i\in\mathcal{N}_j^a$, $\lambda_{jk}^P,\ k\in\mathcal{N}_j^d$, $\lambda_{ij}^Q,\ i\in\mathcal{N}_j^a$, $\lambda_{jk}^Q,\ k\in\mathcal{N}_j^d$, λ_j^v, and $\lambda_i^v,\ i\in\mathcal{N}_j^a$ are the Lagrangian multipliers for the constraints (13f)-(13h) of each bus j. Note that $\mathcal{L}$ is different from the conventional Lagrangian function, where all equality constraints (13f)-(13h) are regularized by the additional quadratic terms. Interestingly, this modification do not change the optimal value [9, 16]. Using the augmented Lagrangian function $\mathcal{L}$, we propose a consensus-based ADMM algorithm to solve (13a)-(13h) that works in an iterative manner. Thanks to the decomposable structure of $\mathcal{L}$, the τ^{th} iteration can be performed locally for each bus j. The details of one iteration is given as follows:

1. Update auxiliary variables: For each bus $j,\ j=1,\dots,N$, its local auxiliary variables $\tilde{P}_{ji}(\tau),\ i\in\mathcal{N}_j^a$, $\tilde{P}_{jk}(\tau),\ k\in\mathcal{N}_j^d$, $\tilde{Q}_{ji}(\tau),\ i\in\mathcal{N}_j^a$, $\tilde{Q}_{jk}(\tau),\ k\in\mathcal{N}_j^d$, $\tilde{v}_{jj}(\tau)$, and $\tilde{v}_{ji}(\tau),\ i\in\mathcal{N}_j^a$ are updated by solving the following optimization problem locally:

$$\min \mathcal{L}_j,\ s.t.\ (13b),(13c),(13d),\text{ and }(13e). \tag{15}$$

where the global variables $P_{ij}(\tau),\ i\in\mathcal{N}_j^a$, $P_{jk}(\tau),\ k\in\mathcal{N}_j^d$, $Q_{ij}(\tau),\ i\in\mathcal{N}_j^a$, $Q_{jk}(\tau),\ k\in\mathcal{N}_j^d$, $v_j(\tau)$, and $v_i(\tau),\ i\in\mathcal{N}_j^a$ used in (15) are fixed and regarded as constant. The solutions of (15) are denoted as $\tilde{P}_{ji}(\tau+1),\ i\in\mathcal{N}_j^a$, $\tilde{P}_{jk}(\tau+1),\ k\in\mathcal{N}_j^d$, $\tilde{Q}_{ji}(\tau+1),\ i\in\mathcal{N}_j^a$, $\tilde{Q}_{jk}(\tau+1),\ k\in\mathcal{N}_j^d$, $\tilde{v}_{jj}(\tau+1)$, and $\tilde{v}_{ji}(\tau+1),\ i\in\mathcal{N}_j^a$.

2. Update global variables: This step updates the global variables $P_{ij},\ i\in\mathcal{N}_j^a$, $P_{jk},\ k\in\mathcal{N}_j^d$, $Q_{ij},\ i\in\mathcal{N}_j^a$, $Q_{jk},\ k\in\mathcal{N}_j^d$, v_j, and $v_i, i\ \in\mathcal{N}_j^a$ used in (15) for each bus $j,\ j=1,\dots,N$:

$$
\begin{aligned}
&P_{ij}(\tau+1)=\frac{1}{2}(\tilde{P}_{ij}(\tau+1)+\tilde{P}_{ji}(\tau+1))\\
&Q_{ij}(\tau+1)=\frac{1}{2}(\tilde{Q}_{ij}(\tau+1)+\tilde{Q}_{ji}(\tau+1))\\
&v_j(\tau+1)=\frac{1}{1+|\mathcal{N}_j^d|}(\tilde{v}_{jj}(\tau+1)+\sum_{k\in\mathcal{N}_j^d}\tilde{v}_{kj}(\tau+1))\\
&P_{ll}=0,Q_{ll}=0,v_{ll}(\tau+1)=\tilde{v}_{ll}(\tau+1),\ l\in\mathcal{T}\\
&P_{01}=\bar{P}_0,Q_{01}=\bar{Q}_0.
\end{aligned}
\tag{16}
$$

Note that $\tilde{P}_{ij}$ ($\tilde{Q}_{ij}$) and $\tilde{P}_{ji}$ ($\tilde{Q}_{ji}$) are different which are the auxiliary variables assigned to the bus i and bus j to estimate the shared global variable P_{ij} (Q_{ij}), respectively. This step requires communication between neighboring buses as the global variables are update by the average of the respective local auxiliary variables of neighboring buses.

3. Update Lagrangian multipliers: The multipliers assigned to each bus $j,\ j=1\dots,N$ are updated linearly by the mismatch of the corresponding consensus constraint:

$$
\begin{aligned}
\lambda_{ji}^P(\tau+1)&=\lambda_{ji}^P(\tau)+\rho_P\left[\tilde{P}_{ji}(\tau+1)\right.\\
&\quad\left.-P_{ij}(\tau+1)\right],\ i\in\mathcal{N}_j^a\\
\lambda_{jk}^P(\tau+1)&=\lambda_{jk}^P(\tau)+\rho_P\left[\tilde{P}_{jk}(\tau+1)\right.\\
&\quad\left.-P_{jk}(\tau+1)\right],\ k\in\mathcal{N}_j^d
\end{aligned}
\tag{17a}
$$

$$
\begin{aligned}
\lambda_{ji}^Q(\tau+1)&=\lambda_{ji}^Q(\tau)+\rho_Q\left[\tilde{Q}_{ji}(\tau+1)\right.\\
&\quad\left.-Q_{ij}(\tau+1)\right],\ i\in\mathcal{N}_j^a\\
\lambda_{jk}^Q(\tau+1)&=\lambda_{jk}^Q(\tau)+\rho_Q\left[\tilde{Q}_{jk}(\tau+1)\right.\\
&\quad\left.-Q_{jk}(\tau+1)\right],\ k\in\mathcal{N}_j^d
\end{aligned}
\tag{17b}
$$

$$
\begin{aligned}
\lambda_{jj}^v(\tau+1)&=\lambda_{jj}^v(\tau)+\rho_v\left[\tilde{v}_{jj}(\tau+1)\right.\\
&\quad\left.-v_j(\tau+1)\right]\\
\lambda_{ji}^v(\tau+1)&=\lambda_{ji}^v(\tau)+\rho_v\left[\tilde{v}_{ji}(\tau+1)\right.\\
&\quad\left.-v_i(\tau+1)\right],\ i\in\mathcal{N}_j^a.
\end{aligned}
\tag{17c}
$$

Since all variables involved in this step have been calculated locally in the previous steps, this step can be realized locally for each bus.

Through the above iterative process, the global optimal solutions can be obtained [9, 16]. Once the algorithm converges, the optimal active and reactive power injection for each bus $j,\ j=1,\dots,N$ can be calculated by (2a) and (2b), i.e., $p_j^\star=\sum_{k\in\mathcal{N}_j^d}\tilde{P}_{jk}^\star-\sum_{i\in\mathcal{N}_j^a}\tilde{P}_{ji}^\star$ and $q_j^\star=\sum_{k\in\mathcal{N}_j^d}\tilde{Q}_{jk}^\star-\sum_{i\in\mathcal{N}_j^a}\tilde{Q}_{ji}^\star$, respectively.

Remark 1. *Note that 1) the power quality management module only takes actions after the command following module is finished, and 2) both modules only take actions after the respective distributed algorithms (i.e., (9) for the command following module and (15)-(17c) for the power quality management module) converge. When implementing the framework in practice, the optimal solutions obtained through the proposed distributed algorithms should meet the requirement of accuracy [2]. In the command following module, for an accuracy level ε_1, the algorithm (9) needs r_0 iterations to converge after which $||\Delta\boldsymbol{p}(r)-\Delta\boldsymbol{p}^*||_2\le\varepsilon_1,\ \forall r>r_0$ where $\Delta\boldsymbol{p}=[\Delta p_1,\dots,\Delta p_N]^T$, $\Delta\boldsymbol{p}^*$ is the optimal solution, and $||\cdot||_2$ denotes the l_2 norm. Thus, the time that it takes for the algorithm (9) to converge is $t_1=r_0\tau_1$ where $\tau_1=r+1-r$ denotes the time scale in the command following module which is close to the calculation time needed for hardware to complete one step*

iteration (millisecond). The similar definition is applied to the algorithm (15)-(17c) in the power quality management module with the accuracy level ε_2, required iteration number τ_0 (after which $||\boldsymbol{x}(\tau) - \boldsymbol{x}^*||_2 < \varepsilon_2$) and required calculation time $t_2 = \tau_0\tau_2$ with time scale τ_2, where $\boldsymbol{x} = [\boldsymbol{p}^T, \boldsymbol{q}^T]^T$ with $\boldsymbol{p} = [p_1, \ldots, p_N]^T$ and $\boldsymbol{q} = [q_1, \ldots, q_N]^T$, and $\boldsymbol{x}^*$ is the optimal solution.

Remark 2. *In the proposed control framework, increasing and decreasing both active and reactive power production of DERs are considered for control purposes. But in most cases, DERs (e.g. photovaltaic) operate in maximum power tracking mode and only deceasing production is allowed. To handle this issue, the whole scheme can be modified to give priority to reactive power adjustment and decrease active generation only if needed. Particularly, 1) in the command following module, the decision variables can change from active power to reactive power of DERs (in this paper, STVC is considered to give active power change command Δp_{ref}, but in our design (e.g., [4]), STVC can also give reactive power change command Δq_{ref}); 2) in the power quality management module, the upper change limit of active power for each DER can set to its maximum power point (which means only deceasing production is allowed) and two new terms related to control cost $||\boldsymbol{p}||_{\Lambda_p}$ and $||\boldsymbol{q}||_{\Lambda_q}$ can be added in the objective, where $||\boldsymbol{p}||_{\Lambda_p} = \boldsymbol{p}^T\Lambda_p\boldsymbol{p}$ (similarly for $||\boldsymbol{q}||_{\Lambda_q}$), the matrices Λ_p and Λ_q are diagonal whose elements are positive, and the diagonal element of Λ_q can be selected much larger than that of Λ_p.*

Remark 3. *The performance of the proposed control framework depends on the availability and quality of the bus-to-bus communication links in distribution networks. So far we assume that these links provide perfect service. Nonetheless, communication link failures may happen in practice, which may have bad effects on the control performance. In the command following module, how the distributed algorithm (9) would handle link failures is still an open question and will be studied in future. In the power quality management module, asynchronous ADMM-based algorithm can be utilized to handle the random communication link failure [9], but how to cope with the permanent link failures for ADMM-based algorithm (15)-(17c) is still an open question, and deserves attention.*

Remark 4. *The ideas presented in this section can be extended to three-phase balanced systems by implementing independent control framework on each phase, i.e., each phase is regarded as an independent DERC. This is realistic since there are commercially available single-phase DERs that are capable of providing both active and reactive power [23]. How to extend the proposed framework to three-phase unbalanced system will be studied in the future.*

4. Case Study

4.1. Test System

The modified IEEE 30-bus test system introduced in [3] is employed to show the effectiveness of the proposed control framework, whose parameters can be found in [3] and network diagram is given in Fig. 2. In the modified IEEE 30-bus test system, there are 15 load buses (buses 1 to 15) in the subtransmission network and each load bus is assumed to have a DERC. In this paper, each DERC is replaced by a distribution network with DERs rather than being treated as an aggregated controller as did in [3].

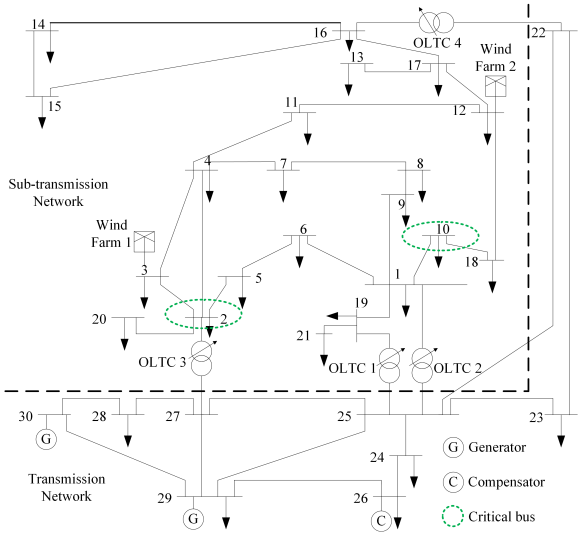

Figure 2: Modified IEEE 30-bus test system

The IEEE 123-bus test feeder [24] is employed to model the distribution network of DERC at load bus 3, whose diagram is given in Fig. 3. And the IEEE 34-bus test feeder [24] is adopted to model the distribution networks of DERCs at the remaining 14 load buses, whose diagram is shown in Fig. 4. To simplify the analysis, the IEEE 123-bus test feeder is modeled as a 4.16 kV single-phase network with $N = 122$, where each line segment has impedance value $(0.17 + j0.17)\ \Omega$, each bus has a constant load of $(30 + j0)$ kVA, and a DER whose active power change limit is $[-20, 20]$ kW and reactive power change limit is $[-100, 100]$ kvar. The IEEE 34-bus test feeder is modeled as a 12 kV single-phase network with $N = 33$, where each line segment has impedance value $(0.23+j0.36)$ Ω, each bus has a constant load of $(50 + j10)$ kVA and a DER whose active power change limit is $[-30, 30]$ kW and reactive power change limit is $[-100, 100]$ kvar.

For the communication network of each distribution network, as mentioned in Section II-B, it has the same topology as the physical grid. In the command following module, each edge $(i, j) \in \mathcal{E}$ is assigned a weight w_{ij} which can be calculated by a simplified computation method: $w_{ij} = \frac{1}{1+\max\{D_i, D_j\}}$ where D_i is the degree of bus i, $i \in \mathcal{N}$.

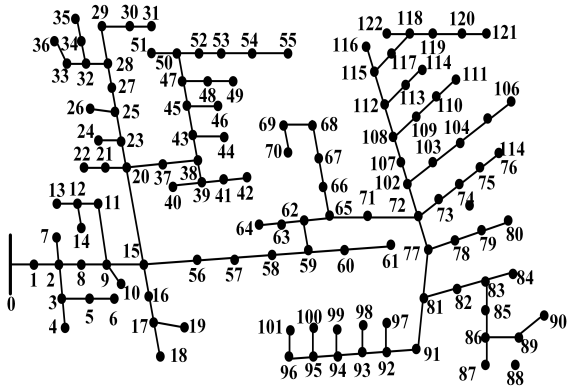

Figure 3: IEEE 123-bus test feeder

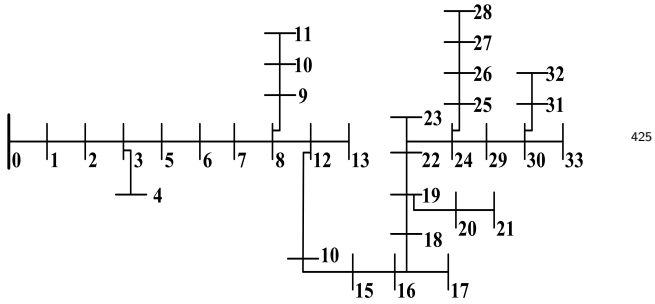

Figure 4: IEEE 34-bus test feeder

4.2. Simulation Results

During the simulation, the STVC proposed in [3] is employed to give the active power change command for each DERC, where DERCs are coordinated with 4 OLTCs and 4 capacitors existed in the subtransmission network. Once each DERC receives the command, its corresponding control framework is activated at once. Each DERC has the following two control objectives:

1. Tracking the active power change command from the STVC quickly.
2. Managing the power quality within the DERC.

In order to test the effectiveness of the proposed control framework, during the simulation, the full ac power flow model, instead of the approximate power flow model (2), is used to model the power flow of real distribution networks. In addition, during the simulation, the taps of the existing OLTCs in each distribution network are held constant for the following reasons: 1) it is assumed that the ability of the DERs to react to voltage violations is faster than that of the OLTCs and 2) the purpose of the case study is to test the control effectiveness of the proposed control framework, so we are interested in studying the ability of our control architecture to correct violations without additional help from the OLTCs.

Table 1: The cost coefficients in the command following module

Bus	a	Bus	a	Bus	a	Bus	a
0	1.176	9	1.009	18	1.105	27	1.010
1	1.176	10	1.197	19	1.051	28	1.012
2	1.058	11	0.887	20	1.109	29	1.144
3	0.992	12	0.842	21	1.173	30	0.994
4	1.056	13	0.844	22	1.189	31	0.957
5	1.018	14	0.825	23	0.877	32	1.069
6	1.059	15	0.962	24	0.856	33	1.097
7	1.018	16	0.979	25	1.079	–	–
8	1.088	17	0.946	26	0.838	–	–

Here are the parameters used in the designed control framework for each DERC in the command following module:

- The cost coefficients of the cost function (3) for IEEE 34-bus feeder are given in Table 1 where $b_i = 0, i \in \mathcal{N}$; the cost coefficients in (3)for IEEE 123-bus feeder are randomly selected in Table 1.
- The step size α is selected as $0.25\sigma_{min}(\tilde{W})\min\{a_i\}$ for IEEE 34-bus feeder and $0.1\sigma_{min}(\tilde{W})\min\{a_i\}$ for IEEE 123-bus feeder.
- The sampling time period τ_1 is selected as 10 ms, which is a typical time needed for commercial off-the-shelf hardware to complete one iteration step [2]; the accuracy level $\varepsilon_1 = 1$ kW for IEEE 34-bus test feeder and $\varepsilon_1 = 2$ kW for IEEE 123-bus test feeder.

For the power quality management module:

- The voltage control limits in (11) are set as $\underline{v}_i = 0.95$ p.u. and $\overline{v}_i = 1.05$ p.u. for each bus i, $i \in \mathcal{N}$.
- The penalty coefficients used in (14b) are selected as $\rho_P = \rho_Q = 0.01$ and $\rho_v = 0.00001$ ($\rho_P = \rho_Q = 0.02$ and $\rho_v = 0.0001$) for IEEE 34-bus feeder (IEEE 123-bus feeder).
- Similar to the command following module, the sampling time period τ_2 is selected as 10 ms; the accuracy level $\varepsilon_2 = 0.1$ ($\varepsilon_2 = 0.2$) p.u. for IEEE 34-bus feeder (IEEE 123-bus feeder).

In the STVC proposed in [3], the 15 DERCs are utilized to help regulate the voltages of two selected critical buses 2 and 10 in the subtransmission network within their respective range [1.0187 1.0227] p.u. and [0.9757 0.9797] p.u. with the high penetration of wind power. The control actions of DERCs are activated at $t = 32, 45, 47$ min. The required active power changes of 15 DERCs at these three time instants can be found in [3]. Fig. 5 (Fig. 6) compares the control performance of the critical bus 2 (bus 10) without and with the proposed control framework. It can be

seen from Fig. 5 and Fig. 6 that both the voltages of the two critical buses can be regulated within the predefined ranges, i.e., the command following module of each DERC achieves the desired control performance.

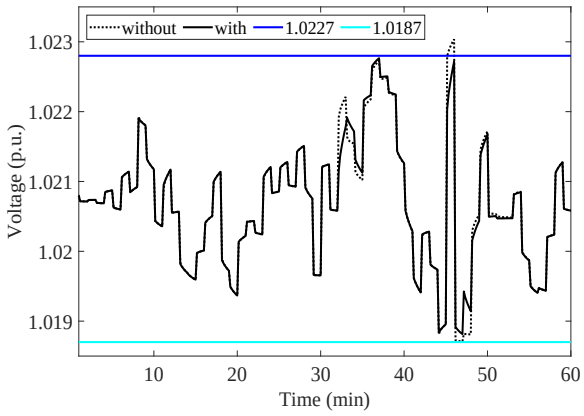

Figure 5: The voltage profile of the critical bus 2

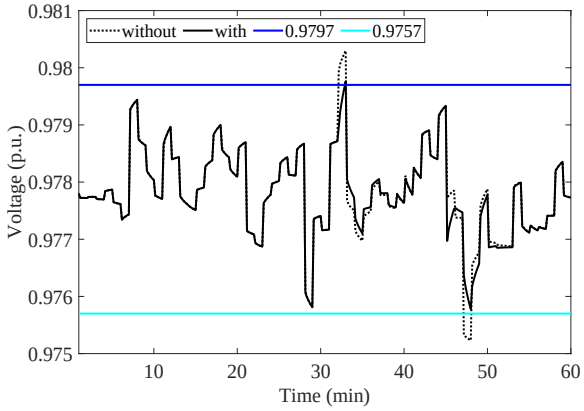

Figure 6: The voltage profile of the critical bus 10

Fig. 7 and Fig. 8 show the decision results and error evolution versus iteration number in the distributed algorithm (9) of the command following module of DERC 10 at $t = 32$ min and DERC 3 at $t = 45$ min, respectively. Note that the overshoot process shown in Fig. 7a and Fig. 8a is caused by the nonlinear projection operator $\mathcal{P}$ in (9) [21], which can not be avoided. It should also be noticed that the overshoot process has no influence on the control performance since the solutions are applied only when the algorithm (9) converges (mentioned in Remark 1). The error is defined as $||\Delta \boldsymbol{p}(r) - \Delta \boldsymbol{p}^*||_2$, where $\Delta \boldsymbol{p}^*$ is the optimal solution obtained through the centralized dispatch with the interior point algorithm. It can be seen from Fig. 7 and Fig. 8 that, given the accuracy level ε_1, the required iteration number $r_0 < 200$, i.e., $t_1 < 2$ s. In the case study, the parameters of the command following module are selected such that the execution time t_1 of each DERC to achieve the accuracy level ε_1 is less than 2 s in all cases, as illustrated in Fig. 5 and Fig. 6, this is short enough to guarantee a desired control performance [3].

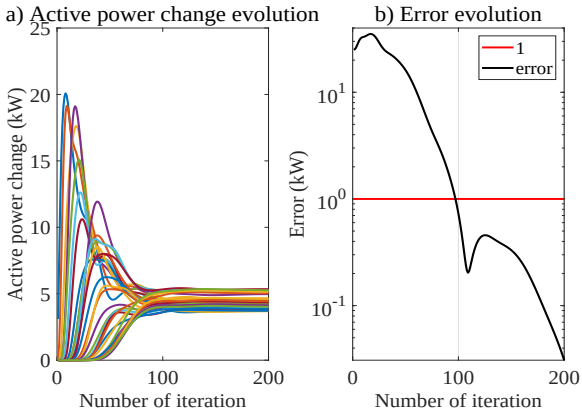

Figure 7: The decision results and error evolution versus iteration number in the distributed algorithm (9) of DERC 10 (IEEE 34-bus feeder) at $t = 32$ min

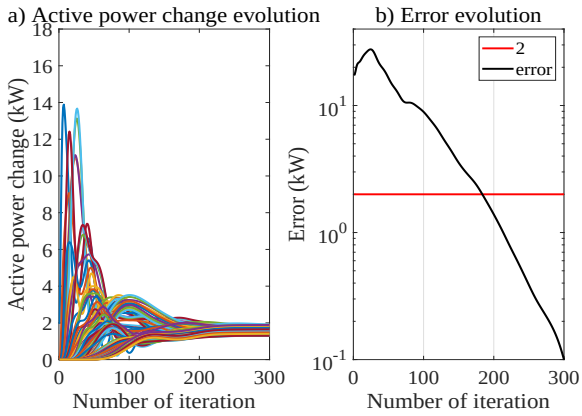

Figure 8: The decision results and error evolution versus iteration number in the distributed algorithm (9) of DERC 3 (IEEE 123-bus feeder) at $t = 45$ min

Fig. 9 and Fig. 10 shows the error evolution versus iteration number in the distributed algorithm (15)-(17c) of the power quality management module of DERC 10 at $t = 32$ min and DERC 3 at $t = 45$ min, respectively. The error is defined as $||\boldsymbol{x}(\tau) - \boldsymbol{x}^*||_2$, where $\boldsymbol{x}^*$ is the optimal solution obtained through the centralized dispatch with the interior point algorithm. It can be seen from Fig. 9 and Fig. 10 that, for the accuracy level ε_2, the required iteration number $\tau_0 < 400$, i.e., $t_2 < 4$ s. In the case study, the parameters of the power management module are selected such that the execution time t_2 of each DERC to achieve the accuracy level ε_2 is less than 4 s in all cases.

We further compare the convergence performance between ADMM-based algorithm (15)-(17c) and dual-ascent algorithm in [13]. Fig. 11 shows the simulation results of DERC 10 (IEEE 34-bus feeder) at $t = 32$ min. It can be seen from Fig. 11 that the convergence speed of our

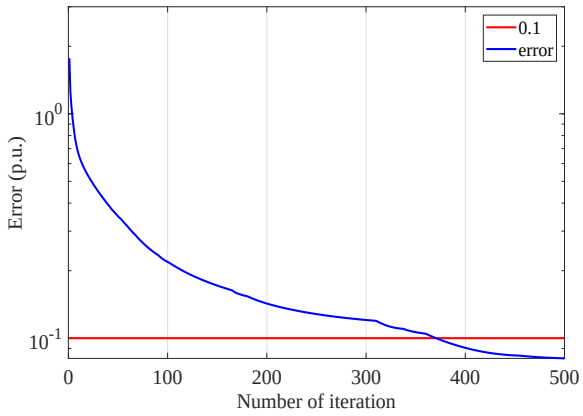

Figure 9: The error evolution versus iteration number in the distributed algorithm (15)-(17c) of DERC 10 (IEEE 34-bus feeder) at $t = 32$ min

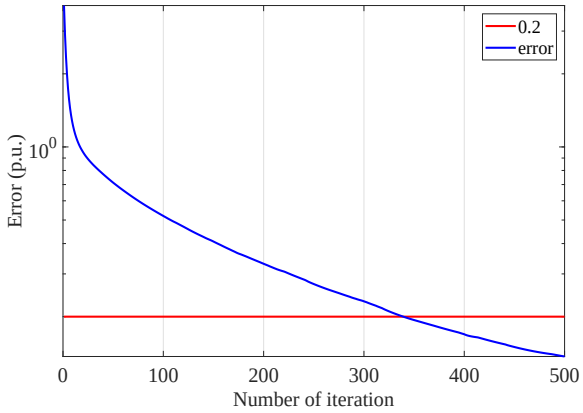

Figure 10: The error evolution versus iteration number in the distributed algorithm (15)-(17c) of DERC 3 (IEEE 123-bus feeder) at $t = 45$ min

proposed ADMM based algorithm is faster than that of dual-ascent method, which demonstrates the advantage of utilizing ADMM in our algorithm.

To demonstrate the effectiveness and importance of the proposed power quality management module, we compare the voltage profile of DERC 10 (DERC 3) without and with the proposed power quality management module at $t = 32$ min ($t = 45$ min). The simulation results are shown in Fig. 12 and Fig. 13. It can be seen from Fig. 12 and Fig. 13 that the voltage violation is avoided when the power quality management module is activated.

5. Conclusions and Future Work

In this paper, a general distributed control framework has been proposed for DERCs to provide voltage support for subtransmission networks. In order to allow a distributed implementation, in the proposed control framework, different distributed control algorithms are constructed for the command following module and the power quality management module, respectively. Through coordination of these two modules, each DERC can quickly track the active power command from the STVC without jeopardizing the power quality at the same time. The effectiveness of the proposed control framework has been tested through a case study with the modified IEEE 30-bus test system.

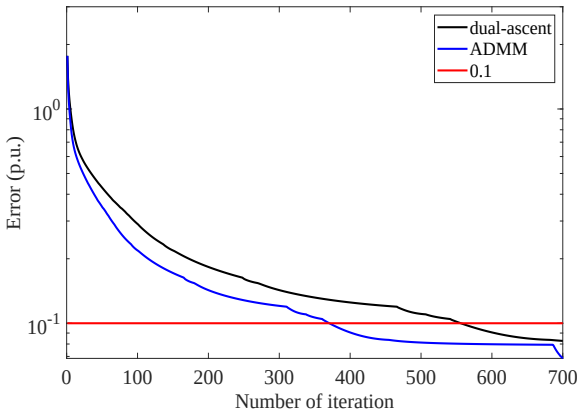

Figure 11: Convergence performance comparison

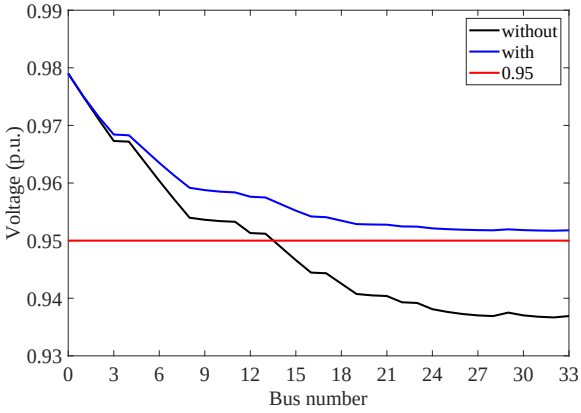

Figure 12: The voltage profile of DERC 10 (IEEE 34-bus feeder) at $t = 32$ min

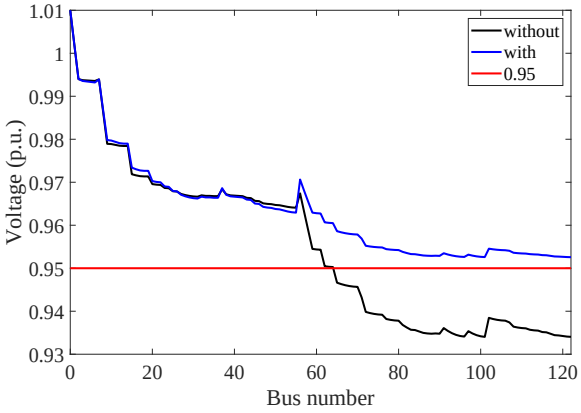

Figure 13: The voltage profile of DERC 3 (IEEE 123-bus feeder) at $t = 45$ min

In the proposed control framework, we only consider the case where the communication links between buses are perfect. An important extension is to cope with the situation where the communication link failure happens. Future works will also concern how to achieve better control performance with distributed algorithms that have very fast convergence speed. In order to better cope with the fast system changes in distribution networks, online algorithms will also be considered for control purpose in future.

6. References

References

[1] S. S. Baghsorkhi, I. A. Hiskens, Impact of wind power variability on sub-transmission networks, in: Proceedings of the IEEE Power and Energy Society General Meeting, 2012, pp. 1–7.

[2] B. A. Robbins, C. N. Hadjicostis, A. D. Domínguez-García, A two-stage distributed architecture for voltage control in power distribution systems, IEEE Transactions on Power Systems, 28 (2) (2013) 1470–1482.

[3] Z. Tang, D. J. Hill, T. Liu, H. Ma, Hierarchical voltage control of weak subtransmission networks with high penetration of wind power, IEEE Transactions on Power Systems, 33 (1) (2018) 187–197.

[4] Z. Tang, D. J. Hill, T. Liu, Fully distributed voltage control in subtransmission networks via virtual power plants, in: Proceedings of the IEEE International Conference on Smart Grid Communications (SmartGridComm), 2016, pp. 193–198.

[5] Z. Tang, D. J. Hill, T. Liu, Two-stage voltage control of subtransmission networks with high penetration of wind power, Control Engineering Practice, 62 (2017) 1–10.

[6] X. Su, M. A. Masoum, P. J. Wolfs, et al., Optimal pv inverter reactive power control and real power curtailment to improve performance of unbalanced four-wire lv distribution networks, IEEE Trans. Sustain. Energy, 5 (3) (2014) 967–977.

[7] M. Farivar, R. Neal, C. Clarke, S. Low, Optimal inverter var control in distribution systems with high pv penetration, in: Proceedings of the IEEE Power and Energy Society General Meeting, 2012, pp. 1–7.

[8] G. Valverde, T. Van Cutsem, Model predictive control of voltages in active distribution networks, IEEE Transactions on Smart Grid, 4 (4) (2013) 2152–2161.

[9] H. J. Liu, W. Shi, H. Zhu, Distributed voltage control in distribution networks: Online and robust implementations, IEEE Transactions on Smart Grid, 9 (6) (2018) 6106–6117.

[10] H. Zhu, H. J. Liu, Fast local voltage control under limited reactive power: Optimality and stability analysis, IEEE Transactions on Power Systems, 31 (5) (2016) 3794–3803.

[11] M. Farivar, L. Chen, S. Low, Equilibrium and dynamics of local voltage control in distribution systems, in: Proceedings of the IEEE 52nd Annual Conference on Decision and Control (CDC), 2013, pp. 4329–4334.

[12] K. Turitsyn, P. Sulc, S. Backhaus, M. Chertkov, Options for control of reactive power by distributed photovoltaic generators, Proceedings of the IEEE, 99 (6) (2011) 1063–1073.

[13] S. Bolognani, R. Carli, G. Cavraro, S. Zampieri, Distributed reactive power feedback control for voltage regulation and loss minimization, IEEE Transactions on Automatic Control 60 (4) (2014) 966–981.

[14] Z. Tang, D. J. Hill, T. Liu, Fast distributed reactive power control for voltage regulation in distribution networks, IEEE Transactions on Power Systems 34 (1) (2018) 802–805.

[15] W. Zheng, W. Wu, B. Zhang, H. Sun, Y. Liu, A fully distributed reactive power optimization and control method for active distribution networks, IEEE Transactions on Smart Grid 7 (2) (2015) 1021–1033.

[16] P. Šulc, S. Backhaus, M. Chertkov, Optimal distributed control of reactive power via the alternating direction method of multipliers, IEEE Transactions on Energy Conversion, 29 (4) (2014) 968–977.

[17] G. Joos, B. Ooi, D. McGillis, F. Galiana, R. Marceau, The potential of distributed generation to provide ancillary services, in: Proceedings of the IEEE Power Engineering Society Summer Meeting, 2000, pp. 1762–1767.

[18] S. Y. Hui, C. K. Lee, F. F. Wu, Electric springs—a new smart grid technology, IEEE Transactions on Smart Grid, 3 (3) (2012) 1552–1561.

[19] M. Baran, F. F. Wu, Optimal sizing of capacitors placed on a radial distribution system, IEEE Transactions on Power Delivery, 4 (1) (1989) 735–743.

[20] M. E. Baran, F. F. Wu, Network reconfiguration in distribution systems for loss reduction and load balancing, IEEE Transactions on Power Delivery, 4 (2) (1989) 1401–1407.

[21] Z. Tang, D. J. Hill, T. Liu, A novel consensus-based economic dispatch for microgrids, IEEE Transactions on Smart Grid, 9 (4) (2018) 3920–3922.

[22] S. Boyd, N. Parikh, E. Chu, B. Peleato, J. Eckstein, et al., Distributed optimization and statistical learning via the alternating direction method of multipliers, Foundations and Trends® in Machine Learning, 3 (1) (2011) 1–122.

[23] "SolarBridge Technologies, Pantheon Microinverter," South Plainfield, NJ, 2009 [online]. Available: http://www.petrasolar.com/.

[24] "IEEE PES Distribution Test Feeders," UWEE, 2009 [online]. Available: http://sites.ieee.org/pes-testfeeders/resources/.